Improving the SO₂ absorption rate of CeFeMg-based sorbent promoted with titanium promoter

Soo Jae Lee***, Soo Chool Lee*, Suk Yong Jung*, Chong Kul Ryu**, and Jae Chang Kim*,†

*Department of Chemical Engineering, Kyungpook National University, Daegu 702-701, Korea
**Korea Electric Power Research Institute, Daejeon 305-380, Korea
***Public & Original Technology Research Center,
Daegu Gyeongbuk Institute of Science and Technology (DGIST), Daegu 704-230, Korea

Abstract−To improve the poor SO₂ absorption rate of CeFeMgTi sorbent with high sulfur removal capacity and fast regeneration, a new sorbent, CeFeMgTi-sol was prepared by the modified co-precipitation method and tested in a packed bed reactor at RFCC conditions (sulfation of MgO to MgSO₄ in the presence of low concentration of SO₂ at 973 K, regeneration of MgSO₄ to MgO and H₂S in the presence of H₂ at 803 K). The CeFeMgTi-sol sorbent showed excellent SO₂ absorption and sulfur removal capacity (46.2 sulfur g/g absorbent×100). It was found that the SO₂ absorption rates were related to the structure of the Mg and Ti and the textural properties such as surface area and pore volume. In the case of the fresh state of CeFeMgTi sorbent, CeO₂, MgO and MgTiO₃ structures were observed. But the new CeFeMgTi-sol sorbent before SO₂ absorption, showed a separated MgO and TiO₂ peak only. These differences in the sorption rates were discussed by the difference in the XRD pattern, surface area and pore volume.

Key words: SO₂, Sorbent, Ce, MgTiO₃, MgO, TiO₂

INTRODUCTION

Sulfur dioxide (SO₂) is a pollutant gas produced by various human activities such as the operation of industrial boilers, the burning of oil and coal at power plants. The discharge of waste gas streams with high levels of toxic compounds into the atmosphere, which is environmentally undesirable, is frequently encountered in conventional operations. In residue fluid catalytic cracking (RFCC) and fluid catalytic cracking (FCC) units, about 45-55% of the sulfur in the hydrocarbon feedstock is converted to hydrogen sulfide in the reactor units and about 35-45% remains as a liquid product. The rest of the sulfur (5-10%) is deposited on the FCC catalyst [1-3]. It has been well known that sulfur can promote the deactivation of cracking catalysts, while the catalytic cracking of hydrocarbons takes place in the reaction zone. Until now, the deactivated catalyst has had to be regenerated in the presence of oxygen in the regeneration bed.

The SO$_x$ emissions, a mixture of 90% of SO₂ and 10% of SO₃, were usually produced from the regeneration units and they had to be removed before their emission entered the atmosphere in order to prevent environmental contamination. To reduce emissions, one or more metal oxides with the absorption capacity of SO$_x$ were added cracking catalysts (1-10 wt%). In RFCC unit, the function of this sorbent is the absorption of SO$_x$ in a catalyst regeneration zone and transformation of SO$_x$ back to H₂S in the cracking reaction zone which can then be treated directly in a Claus plant. The mechanisms generally involve the following reactions:

SO$_x$ (SO₂ and SO₃) is generated from the coke burning in the catalyst regenerator:

$$S(\text{in coke}) + O_2 \rightarrow SO_2 \qquad (1)$$

$$SO_2 + 1/2\,O_2 \rightarrow SO_3 \qquad (2)$$

SO$_x$ is removed by the metal oxide sorbent

$$MeO + SO_2 + 1/2\,O_2 \rightarrow MeSO_4 \qquad (3)$$

$$MeO + SO_3 \rightarrow MeSO_4 \qquad (4)$$

Regenerated in the catalyst reactor:

$$MeSO_4 + 4H_2 \rightarrow MeO + H_2S + 3H_2O \qquad (5)$$

This technique is inexpensive compared with the stack-gas scrubbing or feed hydrodesulfurization techniques and it is, from economical and technical view points, a very practical and attractive technique [2,3]. It is known that basic oxides like magnesium oxide in the presence of an oxidant promoter like CeO₂ have very high potential for SO₂ removal following reactions (1) and (2). Different material promoters such as V, Ce, Co and Pt have been claimed as SO₂ oxidation promoters [4-7], but CeO₂ is the most commonly used today [8-12]. Numerous materials have been proposed for removing SO$_x$. Al₂O₃-based sorbents do not affect the thermal stability of aluminum sulfate in the regeneration condition [6]. MgO-based sorbents have been developed that can absorb SO₂ even at a lower temperature similar to the FCC conditions. Many promoters were added to the MgO in order to promote the SO₂ transformation to SO₃ which would be easily absorbed to the MgO. Even in these cases, however, the MgSO₄ formed during SO₂ absorption is very stable and it has not been completely regenerated under the cracking conditions. Recently, Hydrotalcite type or Magnesium rich hydrotalcite material promoted with various metal oxides such as Ce, Fe, Cu, Mn, Li, Pt and Zn have been used [4,8-10,13-19]. In the previous research, the CeFeMg sorbent showed a high sulfur removal capac-

†To whom correspondence should be addressed.
E-mail: kjchang@knu.ac.kr

ity. However, the sulfur removal capacity of the CeFeMg sorbent was gradually decreased during multiple cycles. To improve this problem, Ti was added into the CeFeMg sorbent by co-precipitation method [20]. The sulfur removal capacity of the CeFeMgTi sorbent was maintained without deactivation even after 8 cycles of sulfation and regeneration unlike the CeFeMg sorbent. However, the SO$_2$ absorption rate of the CeFeMgTi sorbent was slower than those of other sorbents. To solve these problems, the major objectives of this work were to improve the SO$_2$ absorption rate of the CeFeMgTi sorbent by improving the preparation method and physical properties such as surface area and pore volume.

EXPERIMENT

1. Preparation of Sorbent by Coprecipitation Method

1-1. Preparation of CeFeMgTi Sorbent

MgO-based sorbents were prepared by a coprecipitation method. The Ce(NO$_3$)$_3$·6H$_2$O and Fe(NO$_3$)$_3$·9H$_2$O solutions (Ce: 15 wt%) and Fe: 5 wt%) and titanium chloride (Ti: 20 wt%) were added Mg (NO$_3$)$_3$·6H$_2$O having a concentration of 1.5 M solution. The second NaOH solution with a concentration of 1.5 M was added at a flow-rate of 2 mL/min to the metal and Mg solution until the pH value reached 10,5. The resultant gel was aged 18 hrs at 353 K. Then the product was filtered and washed until the pH reached 7. The resultant samples were then dried and calcined in air at 1,023 K for 4 h.

1-2. Preparation of CeFeMgTi-sol Sorbent

The two metal nitrate solutions such as Ce(NO$_3$)$_3$·6H$_2$O and Fe (NO$_3$)$_3$·9H$_2$O of Ce (15 wt%) and Fe (5 wt%) were added to the 1.5 M of magnesium nitrate solution. After mixing for 10 min, NaOH solution (1.5 M) was added to the metals and Mg solution at a flow rate of 2 mL/min, until the pH value reached 10.5. The resultant gel was aged 18 hrs at 80 °C. TiO$_2$ (20 wt%) powder by the sol-gel method was added to the resultant gel prepared previously and this slurry was stirred for 2 hrs. The resultant was filtered and washed until the pH reached 7, then dried and calcined in air at 1,023 K for 4 hrs.

1-3. Preparation of TiO$_2$ by Sol-gel Method

Molar compositions of sec-butanol : Titanium isopropoxide: water= 20 : 1 : 20 were used. Sec-Butanol was mixed with titanium isopropoxide first and then mixed with water. The resultant gel was filtered and washed. Then it was dried and calcined at 773 K for 2 hrs.

1-4. Preparation of Modified Coprecipitation

The MgTi-g (sample b) by modified coprecipitation method was prepared by using the Mg and Ti precipitate pastes. The two pastes was mixed for 1 hour, filtered, washed with deionized water and calcined in the air at 1,023 K for 4 hrs.

2. Apparatus and Procedure

Multiple cycles of sulfidation at 973 K and regeneration at 803 K were performed in a fixed-bed quartz reactor with a diameter of 1 cm in an electric furnace. 0.25 g of sorbent was packed into the reactor and the space velocity (SV) was maintained at 5,000 h^{-1} to minimize severe pressure drops and the channeling phenomenon. All of the volumetric flows of gases were calculated at the standard temperature and pressure (STP) conditions. The temperature of the inlet and outlet lines of the reactor was maintained above 353 K

Table 1. Experimental conditions for MgO-based sorbents

	SO$_2$ absorption		Regeneration	
Temperature (K)	973		803	
Pressure (atm)	1		1	
Flow rate (mL/min)	50		50	
Gas composition	SO$_2$	5000 ppm	H$_2$	50 vol%
	O$_2$	5.2 vol%	N$_2$	balance
	N$_2$	balance		

to prevent condensation of water vapor in the sulfidation processes. The outlet SO$_2$ and H$_2$S gases from the reactor were automatically analyzed every 8 min. By a gas chromatograph (thermal conductivity detector) equipped with an autosampler (Valco). Its detection limitation of SO$_2$ and H$_2$S is about 200 ppm. The column used in the analysis was a 1/8-in. Teflon tube packed with Chromosil 310. The sulfation and regeneration conditions and the composition of mixed gases are shown in Table 1. When SO$_2$ concentration level of the outlet gas reached 5,000 ppm, the concentration of SO$_2$ in the inlet stream of mixed gases, inert nitrogen gas without SO$_2$ was introduced to purge the system, until it reached the regeneration temperature. Sulfurized sorbents were regenerated by the H$_2$ gas until the H$_2$S was not detected.

3. Characterization of Sorbent

The nitrogen adsorption analysis using an Autosorb I (Quantachrome) was used to determine the BET surface area and pore volume characteristic of the sorbent. The 0.2 g sorbent was heated to 673 K at a ramping rate of 1K/min (673 K to 973 K) in 50 mL/min of H$_2$ (50 vol%) and N$_2$ mixture. In addition, in order to identify the crystalline phases of the mixed oxides, an X-ray diffraction (XRD) study was performed with a Philips XPERT instrument using a CuKα radiation source at the Korea Basic Science Institute.

RESULTS AND DISCUSSION

1. SO$_2$ Absorption and Regeneration Performance of CeFe MgTi Sorbent

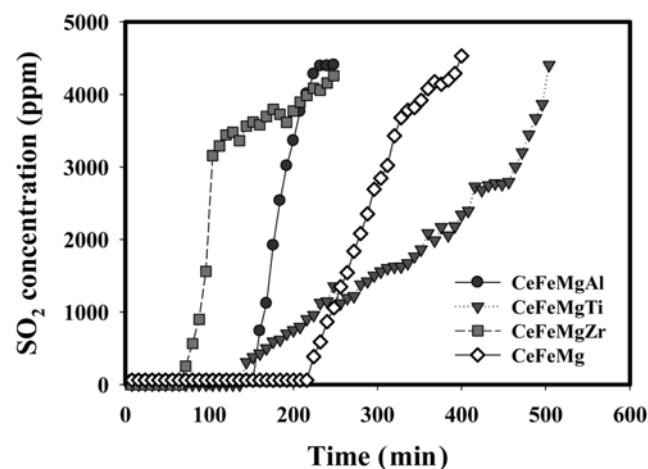The best way to evaluate the absorption capacity of sorbents is

Fig. 1. The SO$_2$ breakthrough curves of CeFeMg-based sorbents promoted with physical promoter such as Al, Ti and Zr.

to determine the so-called breakthrough curves for SO_2 absorption. In a typical fixed-bed experiment, SO_2 concentration of the outlet gas from the reactor is negligible until the entire bed is saturated with sulfur. Fig. 1 shows the breakthrough curves of CeFeMg sorbents and promoted with Zr, Al and Ti sorbents in the first SO_2 absorption. The breakthrough times of these sorbents were 240, 64, 152 and 144 min for CeFeMg, CeFeMgZr, CeFeMgAl and CeFeMgTi,

Table 2. SO₂ removal capacity for various CeFeMg-based sorbent promoted with physical promoter

Sorbent name (wt%)	Sulfur removal capacity
Ce(15)Fe(5)Mg(80)	44.1
Ce(15)Fe(5)MgO(60)Zr(20)	18.1
Ce(15)Fe(5)MgO(60)Al(20)	25.7
Ce(15)Fe(5)MgO(60)Ti(20)	41.20

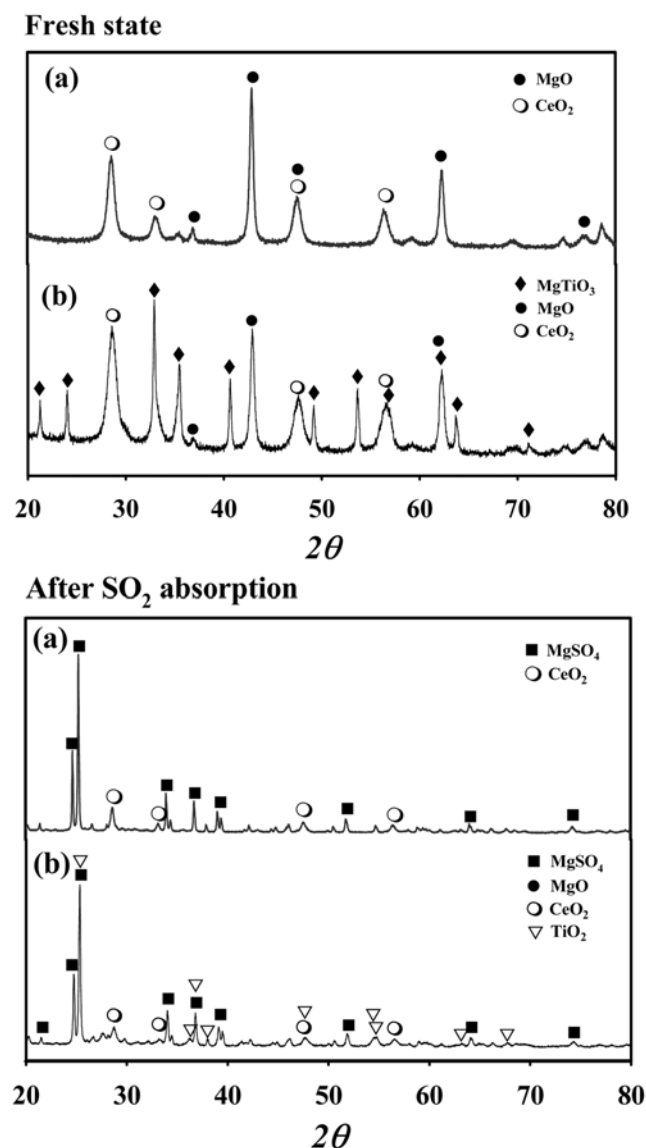**Fresh state**

After SO₂ absorption

Fig. 2. XRD pattern of CeFeMg and CeFeMgTi sorbent before and after SO₂ absorption; (a) CeFeMg, (b) CeFeMgTi.

respectively. In the case of CeFeMgTi sorbent, the breakthrough time was only 144 min, but the inlet SO_2 concentration of outlet gas rose slowly to the SO_2 concentration level. The absorption rate (the absorption amount per time from the breakthrough point to the saturation point) was calculated and the rate of the CeFeMgTi sorbent was slower than those of CeFeMg, CeFeMgZr and CeFeMgAl. The amounts of sulfur absorbed were calculated form SO_2 breakthrough curves. Table 2 shows the amount of sulfur absorbed per gram of sorbent for the CeFeMg sorbent promoted with Zr, Al and Ti. Their sulfur removal capacities were 44.1, 18.1, 25.7 and 41.2 (abs. sulfur g/g absorbent×100) for CeFeMg and CeFeMg promoted with Zr, Al and Ti, respectively. These results indicate that the SO_2 absorption of CeFeMgTi sorbent occurred slowly. Fig. 2 shows the XRD results of CeFeMg and CeFeMgTi sorbents before and after SO_2 absorption. The XRD pattern of CeFeMg sorbent before SO_2 absorption, showed a separated MgO and CeO_2 peak. After SO_2 absorption, all of the separated MgO was transformed to $MgSO_4$. In the case of the fresh state of CeFeMgTi sorbent, CeO_2, MgO and $MgTiO_3$ structures were observed. After SO_2 absorption, MgO and $MgTiO_3$ were transformed to $MgSO_4$ and TiO_2. The decrease in SO_2 the absorption rate of CeFeMgTi sorbent was thought to be due to the formation of the $MgTiO_3$. During the sulfation process, the SO_2 absorption rate is the most important factors to be considered. To increase the SO_2 absorption rate of CeFeMgTi sorbent, the preparation method was modified. The Mg, Fe and Ce gel solutions were prepared by the coprecipitation method, which were mixed with TiO_2 powder by sol-gel method. The resultants were then dried and calcined in air at 750 for 4 hrs. Fig. 3 shows the SO_2 breakthrough curves of CeFeMgTi and the new CeFeMgTi-sol sorbents, when the inlet SO_2 concentration was 5,000 ppm at 973 K. In the case of the CeFeMgTi, The breakthrough time was 108 min. However, the breakthrough time of the new CeFeMgTi-sol sorbent was 200 min and the concentration of breakthrough curve rose rapidly up to the inlet SO_2 concentration. Table 3 shows the amount of sulfur absorbed per gram of sorbent for the CeFeMgTi and the new CeFeMgTi-sol sorbents. Their sulfur removal capacities were 41.2 and 46.2 (abs. sulfur g/g absorbent×100) for CeFeMgTi and CeFeMgTi-sol, respectively. In Table 3, the theoretical sulfur removal capacities were cal-
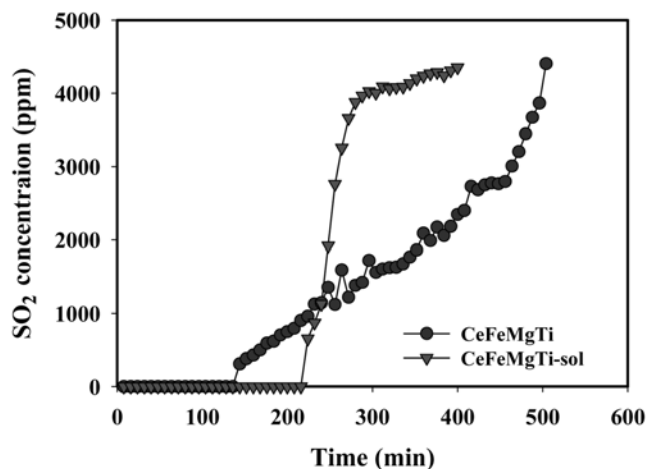

Fig. 3. The SO₂ breakthrough curves of CeFeMgTi and CeFeMgTi-sol sorbents in the first SO₂ absorption process.

Table 3. SO₂ removal efficiency for CeFeMgTi and CeFeMgTi-sol

Sorbent name (wt%)	Theoretical sulfur removal capacity	Sulfur removal capacity	Sulfur removal efficiency (%)
	A	B	B/A×100
Ce(15)Fe(5)Mg(60)Ti(20)	47.68	41.20	86.40
Ce(15)Fe(5)Mg(60)Ti(20)-sol	47.68	46.2	96.9

culated through assuming that only MgO participated in SO₂ absorption and that 1 mole of MgO reacted with the 1 mol of SO₂. In the previous research, the promoted metal oxide such as Ce and Fe oxides were reported to rarely participate in SO₂ absorption [17]. The sulfur-removing efficiency (sulfur removal capacity/theoretical sulfur removal capacity×100) was 85.18% and 96.9% for CeFeMg and CeFeMgTi-sol, respectively. These results indicated that both the sulfur removing capacity and absorption rate of CeFeMgTi-sol were higher than those of CeFeMgTi. The stability during multiple cyclic tests, as well as the sulfur removing capacity, is a very important factor in the RFCC process. When both sulfation and regeneration are considered as a one-cycle process, the sulfur removal capacity of the CeFeMgTi-sol sorbent was 46.2 g sulfur/g absorbent×100 in the first cycle, which was 45.0 g sulfur/g absorbent×100 in the eighth cycles. The sulfur removal capacities of the CeFeMgTi-sol were maintained during multi-cycles.

2. The Characterization of CeFeMgTi-sol and CeFeMgTi

To explain the difference between the SO₂ absorption rate of Ce FeMgTi and that of CeFeMgTi-sol prepared by a new method, XRD pattern, surface area and pore volume were measured. Fig. 4 shows the XRD results of CeFeMgTi-sol sorbent before and after SO₂ absorption. The XRD pattern of CeFeMgTi-sol sorbent before SO₂ absorption, shows separated MgO and CeO₂ peaks. After SO₂ absorption, all of the separated MgO was transformed to MgSO₄. In the previous result, the fresh state of CeFeMgTi would be assigned to CeO₂, MgO and MgTiO₃ structures. After SO₂ absorption, MgO and MgTiO₃ were transformed to MgSO₄ and TiO₂. In addition, after the regeneration process, most of the metal sulfate forms of all the

sorbents were again converted into the initial phases without sulfate forms.

To identify the effect of MgTiO₃ phases on SO₂ absorption rate, two different phases of Mg-Ti-based samples (mol ratio: Mg/Ti=1) were prepared. Sample(a) was prepared by coprecipitation and sample(b) was prepared by modified coprecipitation. Fig. 5 shows the
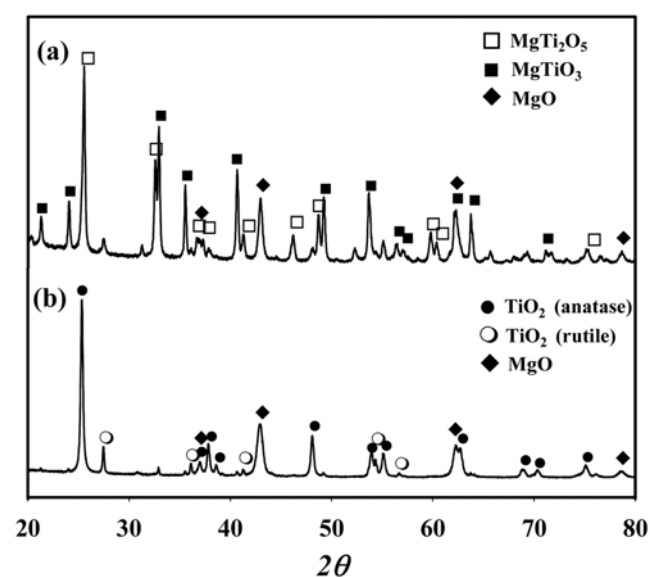

Fig. 5. XRD results of sample(a) and sample(b); sample(a): MgTi₂O₅ and MgTiO₃ phase, sample(b): separated MgO and TiO₂ phase.
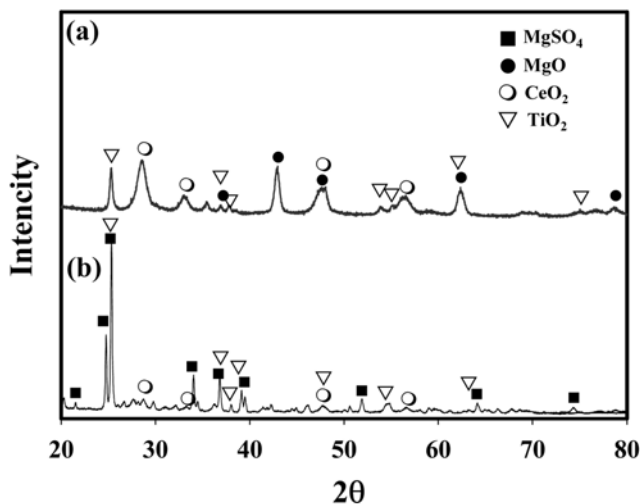

Fig. 4. XRD patterns for the fresh state and after SO₂ absorption of the CeFeMgTi-sol sorbents. (a) Fresh state of CeFeMgTi-sol, (b) After SO₂ absorption.
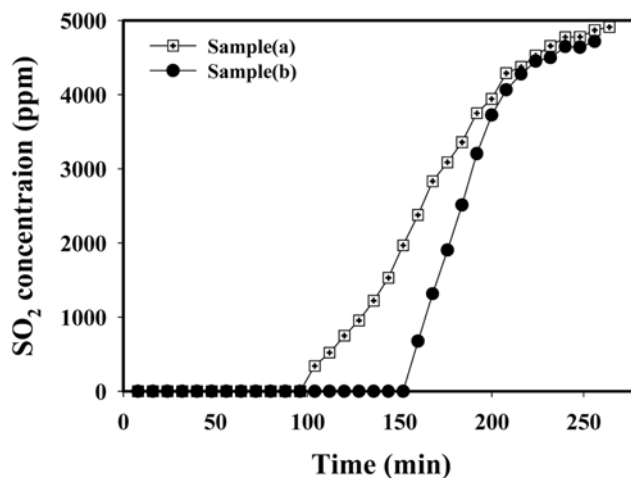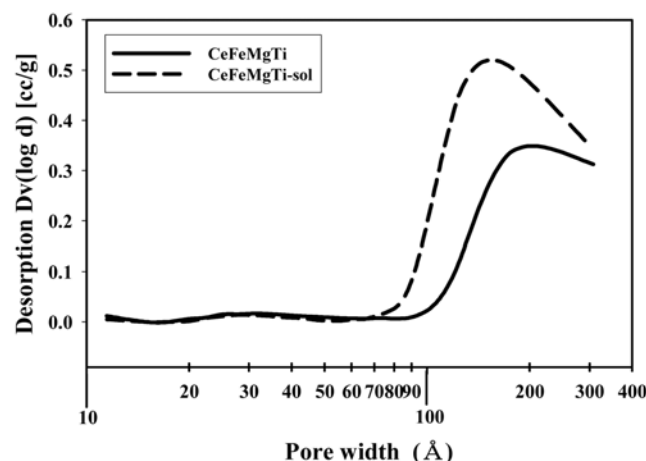

Fig. 6. The SO₂ breakthrough curves for sample(a) and sample(b); sample(a): MgTi₂O₅ and MgTiO₃ phase, sample(b): separated MgO and TiO₂ phase.

Table 4. The physical properties of CeFeMgTi and CeFeMgTi-sol sorbents

Sorbents	Surface area (m²/g)	Total pore volume (mL/g)
CeFeMgTi	41.1	0.1724
CeFeMgTi-gel	62.2	0.2614

Fig. 7. Pore volume of CeFeMgTi and CeFeMgTi-sol sorbents before SO₂ absorption process with pore width.

XRD results of sample(a) and sample(b). The XRD pattern of sample(a) showed the $MgTiO_3$ and $MgTi_2O_5$ peaks. In the case of sample(b) separated MgO and TiO_2 peaks were shown. To investigate the SO_2 absorption performance of sample(a) and (b), 0.2 g of them respectively mixed with 0.05 g of CeO_2 powder. CeO_2 play important catalytic role transforming SO_2 to SO_3 which could be easily absorb SO_2 in MgO. Fig. 6 shows the SO_2 breakthrough curves for sample(a) and sample(b). In the case of sample(a) with structures of $MgTiO_3$ and $MgTi_2O_5$, the breakthrough time was only 92 min and the concentration of the breakthrough curve slowly increased up to the inlet SO_2 concentration. In the case of sample(b) with separated structures of MgO and TiO_2, the breakthrough time was 150 min. The concentration of the breakthrough curve rose rapidly. These results showed that the SO_2 absorption rate of separated MgO and TiO_2 phase is far faster than those of $MgTiO_3$ and $MgTi_2O_5$.

In Table 4, the surface areas of the CeFeMgTi and CeFeMgTi-sol sorbents are 41 m²/g and 62 m²/g, respectively. Fig. 7 shows the pore volume of these sorbents, as a function of pore size. The pore volume of the CeFeMgTi sorbent was about 0.1724 ml/g, while that of the CeFeMgTi-sol sorbent was about 0.2614 ml/g, with the pore size distribution ranging form between 90 and 200 Å. This large surface area and pore volume caused the easy absorption of SO_2. These results indicated that the more rapid SO_2 absorption of CeFeMgTi-sol sorbent was due to separated MgO and TiO_2 phases without formation of the spinel structure and improvement of the textural properties such as surface area and pore volume by the gel-mixing method.

CONCLUSIONS

To improve the SO_2 absorption rate of CeFeMgTi sorbent, a new sorbent (CeFeMgTi-sol) was prepared by a modified co-precipitation method and tested in a fixed bed at RFCC conditions (sulfation 973 K, regeneration 803 K). As a result, the SO_2 absorption rate was found to be dependent on the Mg and Ti phases and physical properties such as surface area and pore volume of the sorbent. In the case of the fresh sorbent of CeFeMgTi, CeO_2, MgO and $MgTiO_3$ structures were observed. The SO_2 absorption rate of the $MgTiO_3$ phase is slower than those of separated MgO supported on TiO_2 phases. The more rapid SO_2 absorption of CeFeMgTi-sol sorbent was due to separated MgO and TiO_2 phases and the improvement of textural properties such as surface area and pore volume by the gel-mixing method. In particular, CeFeMgTi-sol sorbent prepared by the gel-mixing method satisfied the requirement of the SO_2 absorption rate and multiple cycles.

ACKNOWLEDGMENT

REFERENCES

1. J. R. McCauley, US Patent, 5,990,030 (1999).
2. J. A. Wang, L. F. Chen and C. L. Li, *J. Mol. Catal. A*, **139**, 315 (1999).
3. J. A. Wang and C. L. Li, *Appl. Surf. Sci.*, **161**, 406 (2000).
4. J. A. Wang, A. L. Zhu and C. L. Li, *J. Mol. Catal. A*, **139**, 31 (1999).
5. T. Johannessen and S. Koutsopoulos, *J. Catal.*, **205**, 404 (2001).
6. J. Dawody, M. Skoglundh and E. Fridell, *J. Mol. Catal. A*, **209**, 215 (2004).
7. I. Rosso, G. Saracco and V. Specchia, *Korean J. Chem. Eng.*, **20**, 222 (2003).
8. J. S. Yoo, A. A. Bhattacharyya and C. A. Radlowski, *Appl. Catal. B*, **1**, 169 (1992).
9. A. Corma, A. E. Palomares and F. Rey, *Appl. Catal. B*, **4**, 29 (1994).
10. J. S. Yoo, A. A. Bhattacharyya and C. A. Radlowski, *Ind. Eng. Chem. Res.*, **31**, 1252 (1992).
11. J. R. McCauley, US Patent 6,129,833 (2000).
12. J. A. Wang and L. F. Chen, *J. Mol. Catal. A*, **194**, 181 (2003).
13. G. Kim, US patent 5,627,123 (1997).
14. E. W. Albers, US patent 6,338,831 (2000).
15. W. Strehlau. US patent 6,338,945 (2002).
16. S. L. F. Chen, US patent, 6,923,945 (2005).
17. S. J. Lee, H. K. Jun, S. Y. Jung, T. J. Lee, C. K. Ryu and J. C. Kim, *Ind. Eng. Chem. Res.*, **44**, 9973 (2005).
18. M. Cantu, E. L. Salinas and J. S. Valente, *Environ. Sci. Technol.*, **39**, 9715 (2005).
19. S. Y. Jung, H. K. Jun, S. J. Lee, T. J. Lee, C. K. Ryu and J. C. Kim, *Environ. Sci. Technol.*, **39**(23), 9324 (2005).
20. S. J. Lee, S. Y. Jung, S. C. Lee, H. K. Jun, C. K. Ryu and J. C. Kim, *Ind. Eng. Chem. Res.*, accepted.